Contents lists available at ScienceDirect

Physica B: Condensed Matter

Frequency-dependent interface states and diode parameters of Au/n-Si Schottky diode with BOD-Z-EN interfacial layer in dark and under illumination

Ali Osman Tezcan [a], Asrın Baran Çavdar [b], Serkan Eymur [c], Nihat Tuğluoğlu [c,*]

[a] Department of Electricity and Energy, Şebinkarahisar Vocational School, Giresun University, Giresun, Turkey
[b] Department of Mechanical Engineering, Faculty Engineering, Hacettepe University, Ankara, Turkey
[c] Department of Energy Systems Engineering, Faculty of Engineering, Giresun University, Giresun, Turkey

ARTICLE INFO

ABSTRACT

The Au/BOD-Z-EN/n-Si Schottky barrier diode was studied using capacitance/conductance-voltage (C/G-V) and capacitance/conductance-frequency (C/G-f) characteristics under different illumination intensities and in the dark. The increment in C and G at the low-frequency regions, at which the surface states at the semiconductor-organic interface can easily follow the applied ac signal, could be attributed to the surface states. Under illumination, the appearance of peaks in conductance versus logarithm of frequency (G_p/ω- $\log f$) graphs confirmed such interface trap states. It was found that the interface trap density (D_{it}) decreases from 5.81×10^{12} eV^{-1}cm^{-2} to 2.87×10^{12} eV^{-1}cm^{-2} while relaxation time (τ) decreases from 15.76 μs to 3.94 μs with increasing light intensity. The results showed that the barrier height (Φ_B) dropped, going from 0.667 eV (in the dark) to 0.582 eV (100 mW/cm^2). The donor concentration (N_D) rose as the illumination intensity increased, going from 5.46×10^{15} cm^{-3} (in the dark) to 8.08×10^{15} cm^{-3} (100 mW/cm^2).

1. Introduction

The rapid development of semiconductor technology affects the consumer electronic industry and the renewable energy industry [1–4]. In a wide group of semiconductors, recently organic semiconductors have revently attracted great attention due to their characteristic properties, namely mechanical flexibility, low-cost manufacturing processes, and tunable optoelectronic properties [5–11]. These properties make organic semiconductors a promising active material for a new generation of electronic devices, such as thin film transistors, light-emitting diodes, and photovoltaic cells [12–18]. Among others, organic Schottky diodes provide broad application possibilities in high-frequency circuits, optoelectronic systems, and advanced sensors [19–21].

Special features like performance characteristics such as low forward voltage drop, high switching speed, and reduction in power dissipation may be exhibited by the Schottky diodes due to their special combination of metals and semiconductor materials when compared with typical p-n junction diodes [22]. Organic semiconductor materials further enhance these devices, making them an exciting field for electronic and optical interactions. Interactions of light with organic semiconductors can provide deep information about photo-response, charge transport mechanisms, and interface properties due to their possible significant change of electrical properties [23–27].

C-V, and G-V have been widely used to evaluate the performance of Schottky diodes [18,28–32]. Such techniques provide fundamental information on the distribution and behavior of the charge carrier or depletion region or properties of an interface that becomes crucial in determining functionalities. They have also allowed to calculate interface density of states, series resistance can similarly allow a detailed study of the interrelation between the semiconductor and a metal contact. This type of analysis is essential in terms of optimal performance and reliability of the Schottky diodes [33–36].

BODIPY derivatives are well known for excellent photophysical and electronic properties including high fluorescence quantum yields, strong light absorption, and high chemical stability [37–39]. These attributes make BODIPY derivatives highly promising not only as organic semiconductors but also for application in other optoelectronic devices such as organic light emitting diodes, sensors, and photovoltaic cells [40–42]. We took advantage of a BODIPY derivative to serve as the

interfacial material due to its effectiveness in charge transport control and its ability to enhance the interaction between the semiconductor and the interfacial material, thus improving the diode performance under different illumination conditions [43–46].

In our previous work, we used illumination-dependent current-voltage (*I-V*) measurements to examine the Au/BOD-Z-EN/n-Si/In device's electrical and photoelectrical characteristics [47]. The primary goal of this study is to use the conductance approach to ascertain the illumination-dependent distribution and relaxation times of interface trap state (D_{it}) in the Au/BOD-Z-EN/n-Si/In device. The second goal is to assess how light affects the structure's forward and reverse bias *C-V* and *G-V* characteristics while taking the BOD-Z-EN interface layer, D_{it}, and series resistance (R_s) into account. The diode properties, such as donor concentration (N_D) and barrier height (Φ_{C-V}), for each illumination intensity using the reverse bias C^{-2} vs. V plots were also studied. Furthermore, in order to remove the impact of R_s on the capacitance and conductance measurements, the C_m and G_m values obtained at 1 MHz frequency in both dark and illumination intensities were converted to G_c and C_c in order to determine the true values of *G* and *C*.

2. Experimental details

In this study, a phosphorus-doped n-type silicon crystal with a diameter of 2", a thickness of 500 μm, a (100) orientation, and a resistivity of 20 Ω-cm was used as a semiconductor substrate. In our earlier paper, we described the synthesis of the organic material with the chemical formula $C_{25}H_{25}BF_2N_2O$ and the real name ''4,4-difluoro-8-phenyl-1,3,5,7-tetramethyl-6-[(Z)-3-(5-hydroxy-3-ethylpent 3-en-1-yn-1-yl)]-4-bor-3a, 4a-diaza-s-indesen'' named as BOD-Z-EN [47]. The synthesis of BOD-Z-EN was conducted using a well-established protocol as detailed in our previous work [43]. Each batch was verified via spectroscopic techniques (UV–Vis and FTIR) to confirm structural integrity and purity. The Au/BOD-Z-EN/n-Si/In Schottky diode structure was produced employing In metal as the ohmic contact and Au metal as the rectifier contact after the synthesized BOD-Z-EN organic material was placed on the n-Si crystal using the spin coating technique [47]. To ensure reproducibility, each synthesis batch was verified through spectroscopic analysis. The spin-coating deposition parameters (e.g., 2000 rpm for 30 s, 10 mg/mL solution concentration) were optimized in preliminary tests and kept constant for all samples. Electrical measurements performed on multiple diodes fabricated under identical conditions showed consistent behavior, confirming the uniformity of the interfacial layer and its effect on device performance. Fig. 1 displays a schematic diagram of the Au/BOD-Z-EN/n-Si/In diode.

The Keitley 4200A-SCS semiconductor measurement system was used to take the $C-G-V$ and capacitance-conductance-frequency $C-G-f$ measurements that were used to determine the electrical characteristics. The Sciencetech solar simulator was used to create the appli-

cations for illumination intensity. The illumination range of 40–100 mW/cm² was selected based on preliminary tests. Below 40 mW/cm², the device showed minimal response variation, while higher intensities posed risks of thermal effects on the BOD-Z-EN layer. Therefore, the selected range ensured both measurement sensitivity and material stability Voltages ranging from -2 V to +2 V were applied to the diode in order to perform electrical measurements. In the dark, the $C-V$ and $G-V$ measurements were made in the 100 kHz–1 MHz frequency range, while the $C-f$ and $G-f$ measurements were made in the 1 kHz-10 MHz frequency range and the 0–1 V voltage range. While $C-f$ and $G-f$ measurements were made in the frequency range of 1 kHz−10 MHz, $C-V$ and $G-V$ measurements were made at the light source at 1 MHz and at various light intensities of 40, 50, 60, 70, 80, and 100 mW/cm².

3. Results and discussion

3.1. Illumination-dependent capacitance–voltage (C-V) and conductance–voltage (G-V) characteristics

The *C-V* and *G-V* measurements, conducted both in the dark and under varying illumination intensities depending on the frequency and voltage, provide key insights into the electrical properties of the diode. Also, important details regarding the impact of interface states and series resistance on the produced Schottky diodes are provided by the *C-V* and *G-V* measurements. The *C-V* and *G-V* characteristics of Au/BOD-Z-EN/n-Si Schottky diodes were measured in the voltage range of −2 V to +2 V, at a fixed frequency of 1 MHz, and at room temperature, both in the dark and at different light intensities (40, 50, 60, 70, 80, and 100 mW/cm²), and are presented in Figs. 2 and 3, respectively. In the dark and at varying illumination intensities, the examined diode is seen to display the specific MOS-type Schottky diode structure with inversion, depletion, and accumulation areas in Figs. 2 and 3. While the measured *C* and *G* values are nearly constant in the depletion zones, they alter mostly in the accumulation and inversion regions. The conductance value rises and the capacitance value in the accumulation region falls with increasing light intensity.

The effect of illumination on the capacitance characteristic of the diode can be clearly seen in Fig. 2. Under reverse bias, capacitance drops as the depletion width increases steadily, which normally occurs in a diode. Under forward bias, capacitance starts to increase significantly due to carrier injection and accumulation in the organic semiconductor layer. One distinct peak in the forward bias region at nearly 1 V for all illumination conditions is decreasing with an increase in intensity. This
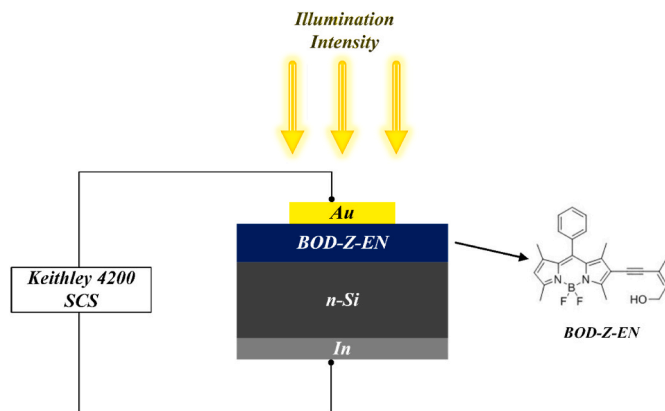

Fig. 1. Schematic structure of the Au/BOD-Z-EN/n-Si/In Schottky diode.
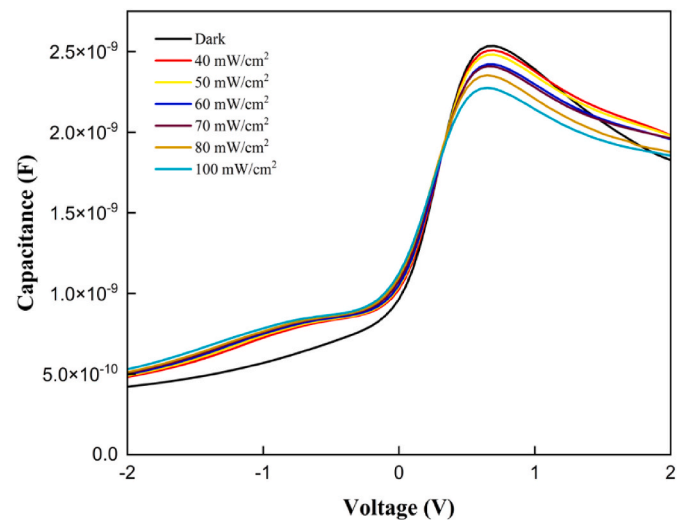

Fig. 2. Measured *C-V* plots of Au/BOD-Z-EN/n-Si Schottky diode in dark and under various illumination intensities.
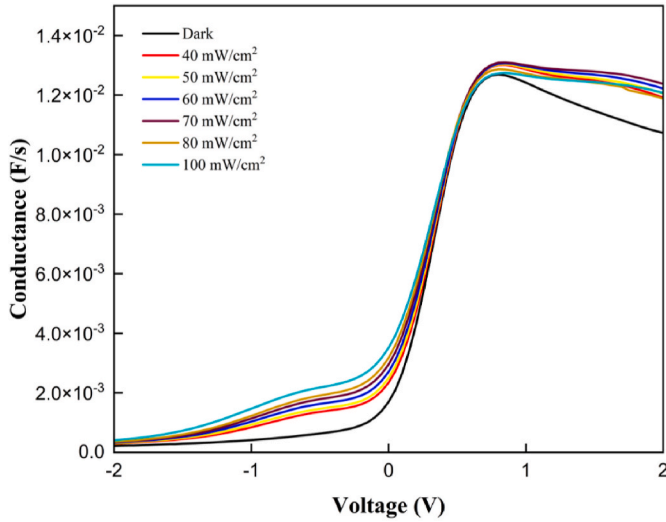
Fig. 3. Measured *G-V* plots of Au/BOD-Z-EN/n-Si Schottky diode in dark and under various illumination intensities.

behavior can be explained by considering that, under increased illumination, a substantial number of electrons from both the valence band and trap states gain sufficient energy to transition into the conduction band. As a result, the overall conductivity of the diode increases while its resistance decreases, in accordance with $G = 1/R$. While interface states are known to influence capacitance and conductance measurements mainly at low frequencies and within the depletion or inversion regions, the series resistance is more dominant in the accumulation region and at high frequencies. Since the *C-V* and *G-V* measurements in this study were performed at 1 MHz, the direct effect of interface states is minimal. Instead, the observed changes in the *C-V* peaks under illumination-both in amplitude reduction and position shift-are primarily attributed to the redistribution of photogenerated carriers at the interface, leading to modifications in the accumulation dynamics.

Measured *G-V* plots of Au/BOD-Z-EN/n-Si Schottky diode in dark and under various illumination intensities are seen in Fig. 3. As evident from Fig. 3 that the conductance increases as the illumination intensity increases. This accounts for the effect of the photogenerated charge carriers on the electrical properties of the diode, indicating that the increase in carrier concentration could lead to variation in the electrical conductivity of the diode. In the reverse bias region, the conductance is low and increases with voltage, consistent with the limited carrier mobility and reduced current flow in this regime. However, under forward bias conditions, a sharp rise in conductance is observed, which becomes more pronounced with higher illumination intensities. This can be attributed to the enhanced carrier injection and recombination dynamics facilitated by the organic semiconductor layer under illumination. The observed plateau of conductance at higher forward bias voltages indicates saturation in carrier injection, where further increase in voltage has a minimal effect on conductance.

The series resistance (R_s) and the interlayer are the sources of "inductive behavior," which refers to the increase in G and the decrease in C in the accumulation region [22,48]. Series resistance (R_s) is only effective in the accumulation zone, but interface states (N_{ss}) are very effective in the depletion and inversion regions [48,49]. To find the R_s of MOS structures, the admittance approach proposed by Nicollian and Brews has been commonly used [22,50]. This method uses the observed *C* and *G* in the strong accumulation region at very high frequencies to determine the real R_s of the MOS structures. The following formula can be used to calculate a MOS type Schottky diode's real R_s [22,50–52]:

$$R_s = \frac{G_m}{G_m^2 + (\omega C_m)^2} \qquad (1)$$

where the measured capacitance, conductance, and angular frequency are denoted by C_m, G_m and ω, respectively.

The $R_s - V$ characteristics of the Au/BOD-Z-EN/n-Si Schottky diode were calculated in the voltage range of -2 V to $+2$ V, at a fixed frequency of 1 MHz, and at room temperature, both in the dark and at different light intensities such as 40, 50, 60, 70, 80, and 100 mW/cm^2, and are shown in Fig. 4. As seen in Fig. 4 that the R_s curves exhibited a maximum in the depletion region and a shift towards the inversion region when seen in the dark and at varying illumination intensities. The series resistance peaks significantly around voltages close to the depletion region at approximately 0 V and then significantly decreases at higher applied forward and reverse bias voltages. This peak is highly affected by illumination intensity; it changes its height and position when operating under various light conditions. For R_s values measured under dark conditions, it was mostly lower in forward and reverse bias regions compared with that measured under illumination. It can be realized that with the increase in the intensity of illumination, the features in R_s become more pronounced, reflecting the enhanced interaction of photo-generated carriers both with the interface states and the bulk of the organic semiconductor layer. The reduction in R_s in the forward bias region upon increased illumination suggests an improvement in charge transportation by the higher density of photo-generated carriers.

The following conversion equations are used to calculate the corrected capacitance (C_c) and conductance (G_c) values in order to eliminate the series resistance effect, which negatively influences the diode's capacitance and conductance measurements [22,50,53]:

$$C_c = \frac{(G_m^2 + \omega^2 C_m^2)C_m}{a^2 + \omega^2 C_m^2}, \ G_c = \frac{(G_m^2 + \omega^2 C_m^2)a}{a^2 + \omega^2 C_m^2}, a = G_m^2 - (G_m^2 + \omega^2 C_m^2)R_s \qquad (2)$$

Fig. 5 shows the corrected $C_c - V$ plots of Au/BOD-Z-EN/n-Si Schottky diode in the dark and under various illumination intensities. It is evident from Figs. 2 and 5 that the C_c values are higher than the C_m values, especially under dark and all lighting conditions. The values of C_c rise to 0.8 V as the forward bias voltage increases, after which they fall to 2.0 V. At 2.0 V for dark and 100 mW/cm^2, the corrected capacitance values of the Schottky diode with BOD-Z-EN interlayer are 3.17 nF and 3.60 nF, respectively. The corrected capacitance shows a clear dependence on applied voltage and illuminating intensity. The capacitance is relatively low in the reverse bias region due to the widening of the depletion region that reduces the density of free carriers. While the
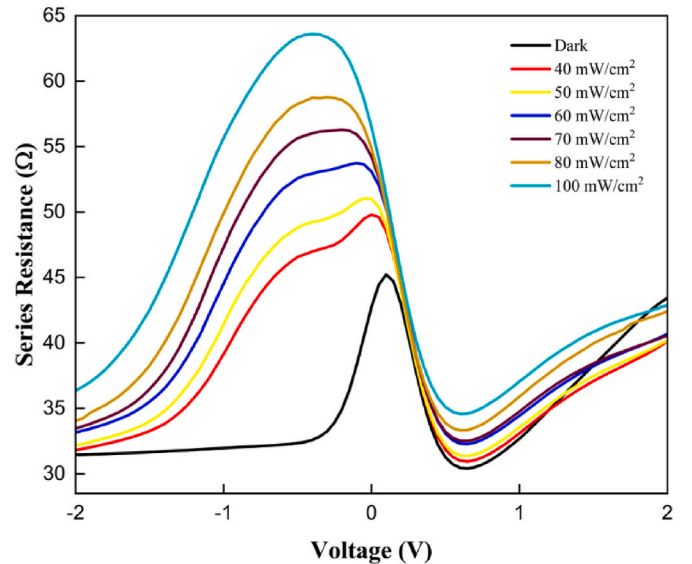

Fig. 4. Calculated $R_s - V$ curves of Au/BOD-Z-EN/n-Si Schottky diode in dark and under various illumination intensities.
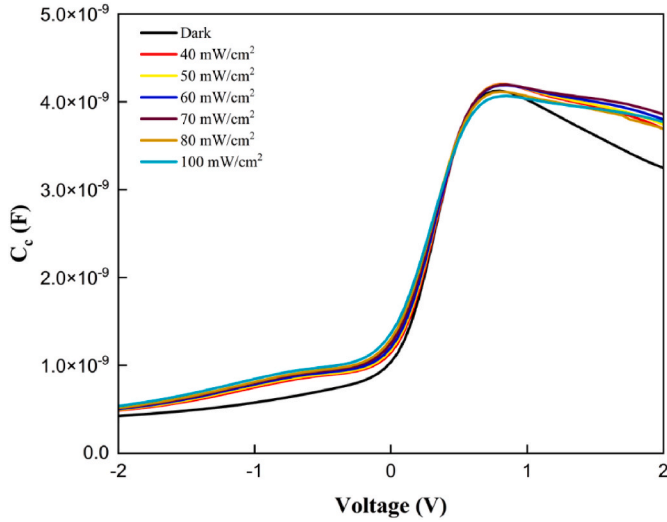
Fig. 5. Corrected $C_c - V$ plots of Au/BOD-Z-EN/n-Si Schottky diode in the dark and under various illumination intensities.

voltage approaches the transition region at approximately 0 V, capacitance increases steeply, with a more significant increase under higher illumination intensities. This increase in the value of C_c upon illumination indicates increased generation and accumulation of charge carriers at the insulator-semiconductor interface. The peak values of capacitance in the forward bias region bring out the effect of photoinduced carriers contributing to an increase in the charge storage capability. This holds good for all the illumination intensities, with higher light intensity levels leading to greater overall capacitance due to increased photo-generated carriers.

Fig. 6 shows the corrected $G_c - V$ plots of Au/BOD-Z-EN/n-Si Schottky diode in the dark and under various illumination intensities. A peak in the depletion zone is visible in the dark and all illumination curves when the diode's corrected conductance curves are analyzed. This peak shifts from 0.25 V for dark to 0.1 V for 100 mW/cm². As the illumination intensity increases, these peaks become more intense. The smooth increase of the corrected conductance with voltage shows a peak in the forward bias region of the conduction mechanism, including the enhancement in the mobility of charge carriers and reduction of barrier resistance in the interface region. The conductance corrected increases systematically with increasing light intensity, as observed by the upward
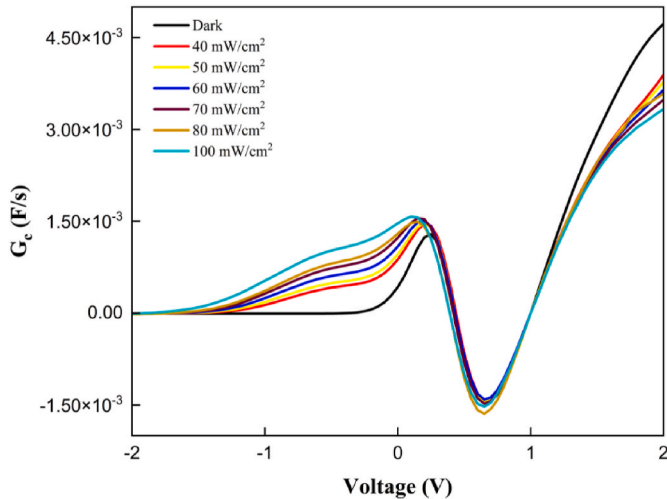
shift of the curves when under illumination. This clearly points to the photoconductive nature of the device, whereby light generates extra carriers and changes the conductivity of the interface. The results consequently underline the role of light in the electrical performance of the diode, featuring an increase in sensitivity and charge transport properties upon illumination.

Additionally, the presence of interfacial state density is indicated by this peak in Fig. 6 [54]. Numerous researchers in the literature have employed the Hill-Coleman approach, which is among the best ways to determine the interfacial state density [54–57]. The values of the interfacial state density of the produced diode can be computed using the peaks of the corrected conductance curve, the depletion area corrected capacitance value, and the following Hill-Coleman equation [54]:

$$D_{it} = \frac{2(G_{c,max}/\omega)}{qA}\left[\left(G_{c,max}/\omega C_{in}\right)^2 + \left(1 - C_c/C_{in}\right)^2\right]^{-1} \qquad (3)$$

where C_{in} is the interface capacitance in the 1 MHz dark curve of $C_c - V$ accumulation area. According to Fig. 5, its value for the Schottky diode with the BOD-Z-EN interlayer was 4.13 nF. The capacitance of the associated conductance peak is denoted by C_c, while $G_{c,max}$ represents the plot's peak value. With the aid of Figs. 5 and 6, the frequency-dependent parameters in Eq. (3) were established for the fabricated Schottky diode and are also included in Table 1. The series resistance (R_s) values at peak voltage were calculated both in the dark and at different illumination intensities and are given in Table 1.

The variations in D_{it} and R_s under various illumination levels and in the dark are depicted in Fig. 7. D_{it} values were determined to be 3.05×10^{11} eV⁻¹cm⁻² for 100 mW/cm² illumination intensity, but they were found to be 2.41×10^{11} eV⁻¹cm⁻² for darkness. For MOS-type Schottky structures, a value of 10^{11} eV⁻¹cm⁻² is optimal [54]. Moreover, the calculated D_{it} values (10^{11} eV⁻¹ cm⁻²) are insufficiently high to pin the Si layer's Fermi level during the device exchange procedure [54]. The reduction in D_{it} and τ with increasing illumination intensity is primarily attributed to the enhanced participation of photogenerated carriers at the interface. These carriers can passivate or fill interface traps, effectively reducing their active density. Moreover, higher carrier injection levels lead to shorter relaxation times due to increased recombination and altered energy levels of traps. Given the photoconductive nature of the BOD-Z-EN interlayer, such behavior is consistent with similar organic-inorganic Schottky structures reported in the literature. Measurement-induced heating effects were minimized through careful experimental controls, and the reliability of frequency-dependent measurements was verified through repeated trials.

3.2. Illumination-dependent capacitance–frequency (C-f) and conductance–frequency (G-f) characteristics

In the illumination intensity range of 0.0–100 mW/cm² at room temperature, the observed capacitance and conductance characteristics of the Au/BOD-Z-EN/n-Si Schottky diode are shown as a function of frequency in Figs. 8 and 9, respectively. Fig. 8 makes it evident that as

Fig. 6. Corrected $G_c - V$ plots of Au/BOD-Z-EN/n-Si Schottky diode in dark and under various illumination intensities.

Table 1
Electrical parameters derived from the Hill-Coleman approach for the Au/BOD-Z-EN/n-Si Schottky diode at the dark and various illumination intensities.

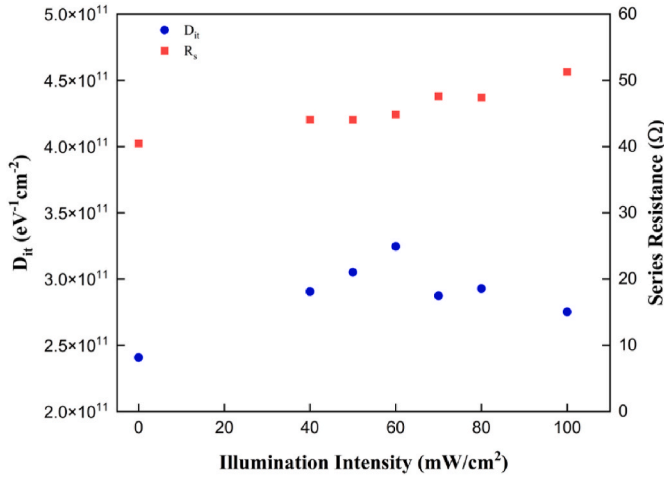| Illumination intensity (mW/cm²)	V_{peak} (V)	$G_{c,max}/\omega$ x 10^{-10} (F)	C_c x 10^{-9} (F)	R_s (at V_{peak}) (Ω)	D_{it} x 10^{11} (eV⁻¹cm⁻²)
0	0.25	2.05	1.74	40.49	2.41
40	0.20	2.31	1.82	44.07	2.91
50	0.20	2.33	1.87	44.05	3.05
60	0.20	2.40	1.90	44.85	3.24
70	0.15	2.46	1.73	47.60	2.87
80	0.15	. 2.37	1.79	47.41	2.92
100	0.10	2.50	1.67	51.29	3.05

Fig. 7. D_{it} and R_s plots of Au/BOD-Z-EN/n-Si Schottky diode in the dark and under various illumination intensities.
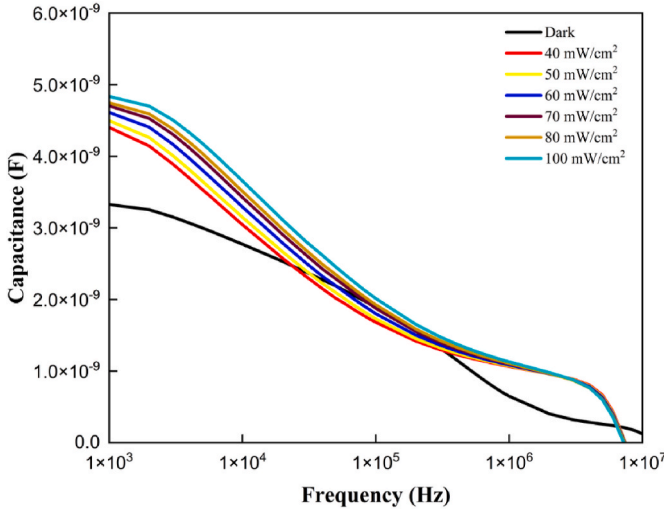

Fig. 8. Measured *C-f* plots of Au/BOD-Z-EN/n-Si Schottky diode in the dark and under various illumination intensities.

frequency increases, the measured capacitance in the depletion area for both dark and all illumination intensity decreases. The excess capacitance caused by the interface state density (D_{it}), which is in equilibrium with the semiconductor that follows the ac signal, was identified as the cause of the high capacitance values at low frequencies [50,56,57]. In other words, in the dark, capacitance shows a continuous decreasing tendency with frequency increase due to an inability of deep interface states to respond to high-frequency signals. Under illumination, capacitance values are higher than that of in the dark especially for the lower frequencies. This points to increased charge storage by photo-generated carriers occupying the interface states. For high frequencies, capacitances tend to merge to the same value for all intensities because only the fast states and bulk can follow rapid changes of the signal.

Fig. 9 makes it evident that, in the lower end of the frequency range, the conductance has been nearly constant up to a specific frequency value. The measurements were made for different illumination intensities: dark and illumination intensities from 40 mW/cm² to 100 mW/cm². It reveals that, in the dark, the conductance increases rather smoothly with frequency without any outstanding peak, hence confirming that when a sample is not under illumination, a minimum photogenerated charge carrier activity occurs. Contrasting results are seen, where clear maxima occur at the peaks in the conductance curves.
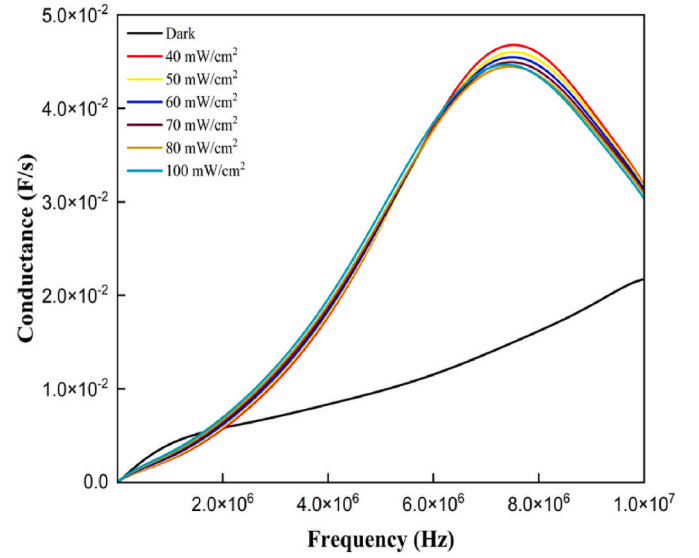

Fig. 9. Measured G-f plots of Au/BOD-Z-EN/n-Si Schottky diode in the dark and under various illumination intensities.

In fact, these peaks seem to slightly shift with the increased light intensity, which also represents an improved interfacial activity when illuminated and consequently enhanced charge carrier activity. It also appears that the conductivity increases with higher light intensity, indicating an increased photogeneration of charge carriers in the diode. Consequently, for the conduction at low frequencies, in all conditions, a low value is maintained, and it might be due to poor response in the conductivity carrier and/or interfacial polarization. Whereas for the higher frequency regime, after the conductance increases to a peak value, it seems to decrease as an effect of poorer charge transport mechanisms or carrier relaxations.

The conductance method introduced by Nicollian and Brews is generally considered the most sensitive and practical means of determining D_{it}. Using this technique, the parallel conductance at a gate bias is measured as a function of frequency and is represented as [54,55]:

$$\frac{G_p}{\omega} = \frac{qD_{it}}{2\omega\tau}ln\left(1+\omega^2\tau^2\right) \tag{4}$$

and can be re-expressed in terms of conductance and capacitance as follows [104,108–110]:

$$\frac{G_p}{\omega} = \frac{\omega G_m C_{in}^2}{G_m^2 + \omega^2(C_{in} - C_m)^2} \tag{5}$$

where $\omega = 2\pi f$ is the angular frequency, D_{it} is the density of the interface states. τ is the relaxation time constant of the interface states.

Fig. 10 depicts the plots of parallel conductance (G_p/ω) versus log f of the Au/BOD-Z-EN/n-Si Schottky diode at dark and various illuminaton intensities. The G_p/ω plots have a peak for dark and each light level, as shown in Fig. 10, and the peak level moves toward higher frequencies as illumination intensity increases. In the dark, there is a pronounced peak at lower frequencies, which indicates the great contribution of interfacial states or defect levels dominating the charge dynamics in the absence of light. Beyond this frequency value, the values fall steeply: therefore, there is low carrier activity and reduced conductivity beyond higher frequencies. When the diode is illuminated, the peak diminishes in magnitude and shifts slightly toward higher frequencies as the light intensity increases. This behavior reflects the generation of photocarriers, which mitigate the dominance of interfacial states observed in the dark. It can also be remarked that, for higher light intensities, the overall values increase in the low-to-mid frequency range, which evidences an increased dynamic response of the diode by
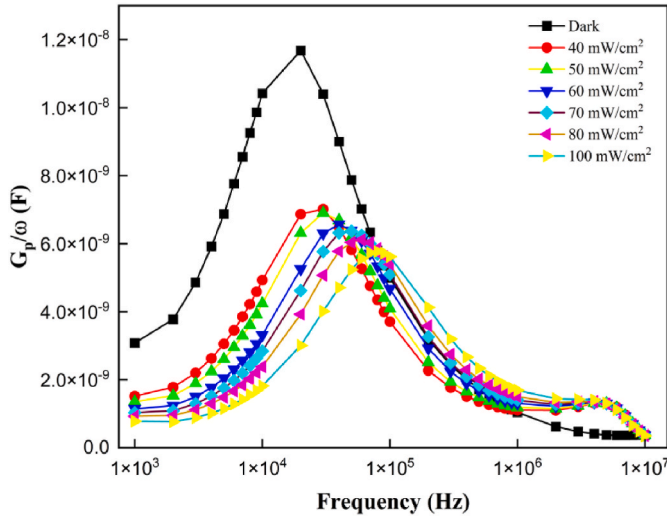
Fig. 10. The Au/BOD-Z-EN/n-Si Schottky diode's equivalent parallel conductance G_p/ω vs frequency at dark and different illumination intensities.

photogenerated carriers.

The following formulas can be used to determine the time constant (τ) and density of the interface states (D_{it}) based on these peak values [58–61]:

$$D_{it} = \frac{(G_p/\omega)_{max}}{0.402qA} \tag{6}$$

$$\tau = 1.98/2\pi f_{max} \tag{7}$$

The frequency at which the G_p/ω peak appears is known as f_{max}. Both the f_{max} value and the D_{it} value that correspond to each $(G_p/\omega)_{max}$ value are found. Both in the dark and with varying illumination intensities, the D_{it} and τ parameters that were computed using Eqs. (6) and (7) and from Fig. 10 are displayed in Fig. 11 and Table 2.

Fig. 11 depicts the illumination intensity distributions of D_{it} for each illumination intensity value between 0 and 100 mW/cm^2 as well as the τ values for each peak frequency. During fabrication operations, these interface states are typically caused by defects such dangling bonds at the interface between the organic semiconductor layer and silicon and energy levels in the semiconductor band gap [62]. Values of D_{it}, represented by the blue circles, are seen to decrease as the intensity of light increases, reflecting that the density of the interface states decreases under higher light exposure. Such behavior could be due to the filling of
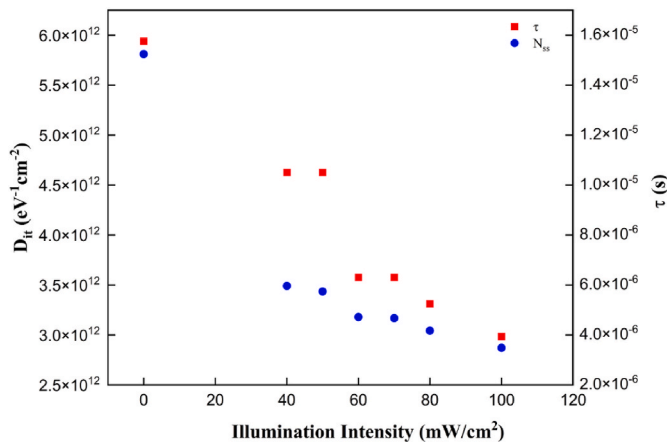

Fig. 11. The interface state density (D_{it}) and relaxation time (τ) vs illumination intensity for the Au/BOD-Z-EN/n-Si Schottky diode.

Table 2

D_{it} and τ parameters calculated using Eqs. (6) and (7) and from Fig. 10 for the Au/BOD-Z-EN/n-Si Schottky diode at dark and various illumination intensities.

Illumination intensity (mW/cm^2)	f_{max} (kHz)	$(G_p/\omega)_{max}$ (nF)	$D_{it} \times 10^{12}$ (eV^{-1}cm^{-2})	τ (μ s)
0	20	11.7	5.81	15.76
40	30	7.02	3.49	10.50
50	30	6.90	3.44	10.50
60	50	6.39	3.18	6.30
70	50	6.37	3.17	6.30
80	60	. 6.12	3.04	5.25
100	80	5.77	2.87	3.94

the interface states or an improvement in charge transport for higher intensities of light. In contrast, the relaxation time τ (red squares) exhibits a more involved behavior: τ decreases with increasing illumination intensity, passes through a minimum, and increases slightly at higher intensities. Such a trend reflects the dynamic recombination processes of carriers at the interface, which is balanced by trap-assisted recombination and generation of charge carriers. According to Table 2 and Fig. 11, D_{it} drops from 5.81×10^{12} eV^{-1} cm^{-2} to 2.87×10^{12} eV^{-1} cm^{-2} when light intensity rises, and τ also drops from 15.76 μs to 3.94 μs at the same period. There is a difference between the D_{it} value obtained from the voltage-dependent measurement and the D_{it} value obtained from the frequency-dependent measurement. This is due to the differences in measurement and calculation methods. Hereby, the specific density distribution in the semiconductor band gap and the different lifetimes of surface states determine their behavior and relaxation time [63].

3.3. Illumination-dependent $1/C^2$-V characteristics

The following relationship describes the depletion layer capacitance in the inversion region of MOS-type Schottky diodes [22,50,64].

$$\frac{d(1/C_c^2)}{dV} = \frac{2}{A^2 \varepsilon_s \varepsilon_0 q N_D} \tag{8}$$

where ε_s is the semiconductor permittivity, A is the area of the Schottky diode, ε_0 is the vacuum permittivity. V_0 and N_D are the intercept voltage and donor concentration which are obtained from the intercept and slope of $1/C_c^2 - V$ curves, respectively.

Some of the fundamental electrical properties of the fabricated MOS-type Schottky diode, including the diffusion potential (V_D), Fermi energy level (E_F), depletion layer width (W_D), and barrier height (Φ_{C-V}), may be found using the following equations:

$$V_D = V_0 + \frac{kT}{q} \tag{9}$$

$$E_F = \frac{kT}{q} ln \frac{N_C}{N_D} \quad ; \quad N_C = 4.82x10^{15} T^{3/2} \left(m_e^*/m_0\right)^{3/2} \tag{10}$$

$$W_D = \sqrt{\frac{2\varepsilon_s \varepsilon_0 V_D}{qN_D}} \tag{11}$$

$$\Phi_{C-V} = V_D + E_F \tag{12}$$

Fig. 12 depicts the reverse-bias $1/C_c^2 - V$ curves for the Au/BOD-Z-EN/n-Si Schottky diode in the illumination intensity range of 0–100 mW/cm^2 that were determined from the data of Fig. 5. Fig. 12 shows that the curves in the depletion area of the Au/BOD-Z-EN/n-Si Schottky diode are linear at dark and various illumination intensities. Using the cut-off point of reverse bias $1/C_c^2 - V$ curves for Au/BOD-Z-EN/n-Si Schottky diode in the illumination intensity range of 0–100 mW/cm^2, the diffusion potential (V_D), Fermi energy level (E_F), depletion layer width (W_D), and barrier height (Φ_{C-V}) parameters were computed and
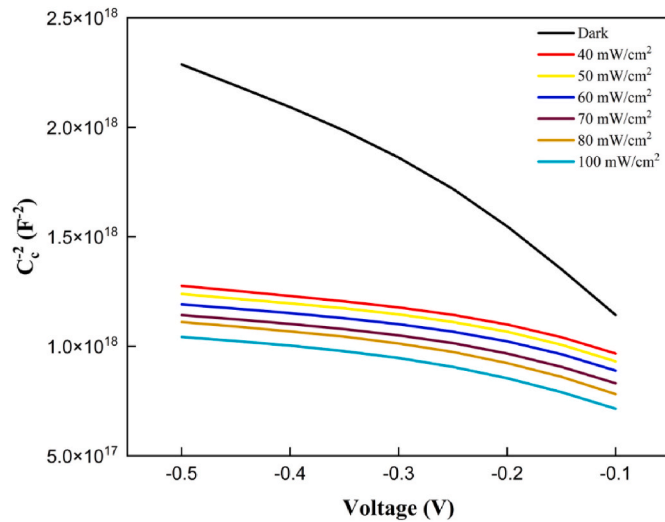
Fig. 12. $C_c^{-2} - V$ curves of Au/BOD-Z-EN/n-Si Schottky diode in the dark and under various illumination intensities.

are shown in Table 3. Table 3 shows that the diffusion potential (V_D), Fermi energy level (E_F), depletion layer width (W_D), and barrier height (Φ_{C-V}) parameters were computed as 0.471 V, 0.195 eV, 3.358 × 10^{-5} cm, and 0.667 eV in the dark, respectively, while they were found to be 0.396 V, 0.185 eV, 2.531 × 10^{-5} cm, and 0.581 eV at 100 mW/cm^2 light intensity.

4. Conclusions

In this work, the capacitance and conductance measurements of Au/BOD-Z-EN/n-Si Schottky diode are taken under dark, in the illumination range of 40–100 mW/cm^2, in the voltage range of - 2 V to +2 V and from 1 kHz to 10 MHz. The diode's *C-V* characteristics in the absence of light and under varying illumination levels exhibit reverse inversion, depletion, and accumulation areas, which are features of MOS-type diodes. The Hill-Coleman approach was used to analyze the illumination-dependent distribution of D_{it}, while the Nicollian and Brews method was used to evaluate the R_s distribution. In the dark and at all illumination intensities, the capacitance values of Au/BOD-Z-EN/n-Si Schottky diodes declined as the frequency increased. As the frequency rises, this decrease makes it impossible for the carriers to follow the signal, which lowers the diode capacitance. The parallel conductance approach, which efficiently calculates the D_{it} and τ, was used to determine the distributions of interface state intensities (D_{it}) and their relaxation times (τ). The values of the τ and D_{it} at dark and in 100 mW/cm^2 varied between 15.76 μ s - 5.81 × 10^{12} eV^{-1} cm^{-2} and 3.94 μ s – 2.87 × 10^{12} eV^{-1} cm^{-2}, respectively. The density of the interface state was found to be suitable for electronic device technology, falling within the range of 10^{11}-10^{12} eV^{-1} cm^{-2}. Furthermore, the reverse bias capacitance graphs for dark and each illumination intensity were also used to determine the doping donor atoms (N_D) and barrier height Φ_{C-V} values.

CRediT authorship contribution statement

Ali Osman Tezcan: Writing – review & editing, Writing – original draft, Methodology, Formal analysis. **Asrın Baran Çavdar:** Writing – review & editing, Writing – original draft, Methodology, Formal analysis. **Serkan Eymur:** Writing – review & editing, Writing – original draft, Methodology, Formal analysis, Conceptualization. **Nihat Tuğluoğlu:** Writing – review & editing, Writing – original draft, Project administration, Methodology, Investigation, Formal analysis, Conceptualization.

Table 3
Illumination-dependent electrical parameters of Au/BOD-Z-EN/n-Si Schottky diode using reverse bias $C_c^{-2} - V$ characteristics.

Illumination intensity (mW/cm^2)	V_D (V)	N_D x 10^{15} (cm^{-3})	E_F (eV)	W_D x10^{-5} (cm)	Φ_{C-V} (eV)
0	0.471	5.457	0.195	3.358	0.667
40	0.554	8.054	0.185	2.997	0.739
50	0.522	7.926	0.186	2.931	0.707
60	0.504	8.054	0.185	2.858	0.689
70	0.466	8.032	0.185	2.754	0.652
80	0.422	. 7.812	0.186	2.655	0.608
100	0.396	8.081	0.185	2.531	0.582

Data availability

The authors of this study declare that the data that supports their findings is available within the paper. The datasets that were generated and/or analyzed during the study are also available from the corresponding author upon reasonable request.

Declaration of competing interest

The authors declare that they have no known competing financial interests or personal relationships that could have appeared to influence the work reported in this paper.

Data availability

The data that has been used is confidential.

References

[1] S.J. Moloi, J.O. Bodunrin, Characterisation of interface states of Al/p-Si Schottky diode by current-voltage and capacitance-voltage- frequency measurements, J. Mater. Sci. Mater. Electron. 34 (2023) 1712.

[2] S. Bengi, S. Altindal, S. Zeyrek, *Determining the dielectric characteristics of the Au/ C20H12/n-Si (MPS) structure over a wide temperature and voltage*, Indian J. Phys. 98 (2024) 2039–2046.

[3] A. Mutlu, M. Can, C. Tozlu, SAM-mediated interface engineering for enhanced Schottky diode characteristics, J. Mater. Sci. Mater. Electron. 35 (2024) 2275.

[4] A.M. Hassanien, A.A.A. Darwish, A.M. Kamal, Spectroscopic and electronic investigations on tin(II) 2,3-naphthalocyanine/p-Si heterojunction for optoelectronic applications, Phys. Scripta 99 (2024) 055532.

[5] H.H. Gullu, D.E. Yildiz, L. Toppare, A. Cirpan, Electrical characteristics of organic heterojunction with an alternating benzotriazole and fluorene containing copolymer, J. Mater. Sci. Mater. Electron. 31 (2020) 18816–18831.

[6] S. Çavdar, P. Oruç, S. Eymur, N. Tugluoglu, Frequency-dependent capacitance and conductance characteristics and current transport mechanisms of Schottky diodes with TPA-IFA organic interfacial layer, Phys. Scripta 99 (2024) 095986.

[7] A.G. Imer, E. Kaya, A. Dere, A.G. Al-Sehemi, et al., Illumination impact on the electrical characteristics of Au/Sunset Yellow/n-Si/Au hybrid Schottky diode, J. Mater. Sci. Mater. Electron. 31 (2020) 14665–14673.

[8] S. Çavdar, P. Oruc, S. Eymur, N. Tugluoglu, Investigation of photosensitive and photodetector characteristics of n-TPA-IFA/p-Si heterojunction structure, J. Mater. Sci. Mater. Electron. 35 (2024) 1022.

[9] P. Oruc, S. Eymur, N. Tugluoglu, Investigation of Terp-Pyr/p-Si diode using complex impedance spectroscopy depending on measurement temperatures and frequencies, J. Mater. Sci. Mater. Electron. 35 (2024) 314.

[10] B. Baris, H.G. Özdemir, N. Tugluoglu, S. Karadeniz, et al., Optical dispersion and dielectric properties of rubrene organic semiconductor thin film, J. Mater. Sci. Mater. Electron. 25 (2014) 3586–3593.

[11] S. Izmirli, S. Cavdar, O. Dos, H. Koralay, N. Tugluoglu, Dielectric properties and electrical characteristics of a triphenylamine thin film deposited onto a silicon substrate via spin coating, ACS Appl. Electron. Mater. 6 (2024) 5057–5066.

[12] F.S. Kaya, Determination of temperature and light intensity on the Ni/chlorophyll-a/n-GaP device, J. Phys. Chem. Solid. 183 (2023) 111656.

[13] M.A. Ibrahim, A. Badran, S.A. Halim, N. Roushdy, A.A.M. Farag, Enhanced structural and optical performance of the novel 3- (5-amino-1-phenyl-1-pyrazol-4-

yl)carbonyl -1-ethyl-4-hydroxyq uinolin-2(1)-one heterojunction: experimental and DFT modeling, Opt. Quant. Electron. 56 (2024) 257.

[14] M. Can, A.K. Havare, OLED application of π-conjugated phenylimino carboxylic acid organic semiconductor material, Eur. Phys. J. Appl. Phys. 97 (2022) 33.

[15] O.H. Mahmood, A. Ugur, A.G. Imer, The photodetection characteristics of a Brilliant Blue-FCF implemented device for organic-based optoelectronic applications, J. Phys. Chem. Solid. 184 (2024) 111733.

[16] M.C. Bodur, S. Duman, I. Orak, S. Saritas, O. Baris, The photovoltaic and photodiode properties of Au/Carmine/n-Si/Ag diode, Opt Laser. Technol. 162 (2023) 109251.

[17] S. Izmirli, S. Cavdar, P. Oruc, S. Eymur, N. Tugluoglu, Impact of voltage and frequency on electrical characteristics of MIS capacitors with triphenylamine layer, Physica B 696 (2025) 416606.

[18] G. Özel, S. Demirezen, Investigation of hybrid CuPc-doped ZnO/p-silicon photodiodes for photonic and electronic applications, J. Mater. Sci. Mater. Electron. 35 (2024) 946.

[19] G.H. Ibrahim, U. Zschieschang, H. Klauk, L. Reindl, High-frequency rectifiers based on organic thin-film transistors on flexible substrates, IEEE Trans. Electron. Dev. 67 (2020) 2365–2371.

[20] E.F.M. El-Zaidia, A.A.A. Darwish, I.S. Yahia, Rhodamine-6G organic films for optical limits: structural analysis, surface morphology, linear and nonlinear optical characteristics, Eur. Phys. J. Plus 136 (2021) 422.

[21] S. Demirezen, S. Altındal Yeriṣkin, A detailed comparative study on electrical and photovoltaic characteristics of Al/p-Si photodiodes with coumarin-doped PVA interfacial layer: the effect of doping concentration, Polym. Bull. 77 (2020) 49–71.

[22] E.H. Rhoderick, R.H. Williams, Metal-semiconductor Contacts, Clarendon Press, 1988.

[23] A.A.A. Darwish, E.A.A. El-Shazly, A.A. Attia, K.F. Abd El-Rahman, *Dark electrical properties and photovoltaic performance of organic/inorganic (SnPcCl2/p-Si) solar cells*, J. Mater. Sci. Mater. Electron. 27 (2016) 8786–8792.

[24] S. Abu Alrub, A.I. Ali, R.K. Hussein, S.K. Alghamdi, S.A. Eladly, DFT and TD-DFT investigations for the limitations of lengthening the polyene bridge between N,N-dimethylanilino donor and dicyanovinyl acceptor molecules as a D-π-A dye-sensitized solar cell, Int. J. Mol. Sci. 25 (2024) 5586.

[25] A.H. Ammar, M.S. Mozdad, M.A. Gouda, Insights into electrical dynamics: alternating current conductivity and impedance spectroscopy in 2-cyano-N-(9,10-dioxo-9,10-dihydroanthracen-2-yl)-2-(2-phenylhydr azono)acetamide, Appl. Phys. A 130 (2024) 914.

[26] A. Naguib, A.M. Elseman, E.A. Ishak, M.S.A. El-Gaby, Novel hole transport materials of pyrogallol-sulfonamide hybrid: synthesis, optical, electrochemical properties and molecular modelling for perovskite solar cells, Mater. Renew. Sustain. Energy 14 (3) (2025).

[27] S. Cavdar, S. Izmirli, H. Koralay, N. Turan, et al., Optoelectronic properties of triphenylamine organic thin film layered Al/p-Si/TPA/Al heterojunction for photodiode application, ECS J. Solid State Sci. Technol. 12 (2023) 045001.

[28] H. Tecimer, S.O. Tan, S. Altindal, Frequency-dependent admittance analysis of the metal-semiconductor structure with an interlayer of Zn-doped organic polymer nanocomposites, IEEE Trans. Electron. Dev. 65 (2018) 231–236.

[29] M. Yilmaz, A. Kocyigit, S. Aydogan, U. Incekara, et al., Light-sensing behaviors of organic/n-Si bio-hybrid photodiodes based on malachite green (MG) organic dye, J. Mater. Sci. Mater. Electron. 31 (2020) 21548–21556.

[30] M.A. Manthrammel, I.S. Yahia, M. Shkir, S. AlFaify, et al., Novel design and microelectronic analysis of highly stable Au/Indigo/n-Si photodiode for optoelectronic applications, Solid State Sci. 93 (2019) 7–12.

[31] S.A. Al-Ghamdi, T.A. Hamdalla, E.F.M. El-Zaidia, A.O.M. Alzahrani, et al., Structural, electronic, and optoelectronic characteristics of GaClPc/n-Si heterojunction for photodiode device, Mater. Sci. Semicond. Process. 147 (2022) 106704.

[32] Ç.Ş. Güçlü, E.E. Tanrıkulu, M. Ulusoy, Y.A. Kalandargh, Ş. Altındal, Frequency-dependent physical parameters, the voltage-dependent profile of surface traps, and their lifetime of Au/(ZnCdS-GO:PVP)/n-Si structures by using the conductance method, J. Mater. Sci. Mater. Electron. 35 (2024) 348.

[33] N. Kaplan, E. Tasci, M. Emrullahoglu, H. Gökce, et al., Analysis of illumination dependent electrical characteristics of α- styryl substituted BODIPY dye-based hybrid heterojunction, J. Mater. Sci. Mater. Electron. 32 (2021) 16738–16747.

[34] A.R. Deniz, A.I. Tas, Z. Çaldiran, Ü. Incekara, et al., Effects of PEDOT:PSS and crystal violet interface layers on current-voltage performance of Schottky barrier diodes as a function of temperature and variation of diode capacitance with frequency, Curr. Appl. Phys. 39 (2022) 173–182.

[35] M.F. Sahin, E. Tasci, M. Emrullahoglu, H. Gökce, et al., Electrical, photodiode, and DFT studies of newly synthesized π-conjugated BODIPY dye-based Au/BOD-Dim/n-Si device, Physica B 614 (2021) 413029.

[36] K. Yıldız, A. Khalkhali, A. Uzun, E. Erbilen Tanrıkulu, et al., The investigation of main electrical parameters, energy dependent profiles of surface states and their lifetimes in the Au/n-Si Schottky diodes with (PVA-Fe3O4) interlayer depend on frequency and voltage, Phys. Scripta 100 (2025) 0159a1.

[37] J. Ordóñez-Hernández, J.G. Planas, R. Núñez, Carborane-based BODIPY dyes: synthesis, structural analysis, photophysics and applications, Front. Chem. 12 (2024) 1485301.

[38] Ö. Sevgili, L.B. Tasyürek, S. Bayindir, I. Orak, E. Caliskan, The current transformer mechanism and structural properties of novel Al/BODIPY/pSi and Au/BODIPY/pSi heterojunctions, Mater. Sci. Semicond. Process. 130 (2021) 105805.

[39] S. Duman, E.Y. Gül, M. Aydemir, H. Selvitopi, et al., Enhanced photodiode performance: Au/boron-dipyrromethene/n-Si/Ag structure unveiling high photosensitivity and efficiency, Opt Laser. Technol. 181 (2025) 11648.

[40] S. Kolemen, Y. Cakmak, T. Ozdemir, S. Erten-Ela, et al., Design and characterization of Bodipy derivatives for bulk heterojunction solar cells, Tetrahedron 70 (2014) 6229–6234.

[41] L. Wang, M.H. Zhu, T.T. Gu, X. Liang, et al., Dimeric BODIPY donors based on the donor-acceptor structure for all-small-molecule organic solar cells, ACS Appl. Energy Mater. 7 (2024) 11195–11205.

[42] E.A. Yildiz, G. Sevinc, H.G. Yaglioglu, M. Hayvali, Strategies towards enhancing the efficiency of BODIPY dyes in dye sensitized solar cells, J. Photochem. Photobiol., A A 375 (2019) 148–157.

[43] E.A. Yildiz, G. Sevinc, H.G. Yaglioglu, M. Hayvali, The effect of molecular structure and ultrafast electron injection dynamics on the efficiency of BODIPY sensitized solar cells, Opt. Mater. 91 (2019) 50–57.

[44] O. Ongun, E. Tasci, M. Emrullahoglu, Ü. Akin, et al., Fabrication, illumination dependent electrical and photovoltaic properties of Au/BOD-Pyr/n-Si/In Schottky diode, J. Mater. Sci. Mater. Electron. 32 (2021) 15707–15717.

[45] A. Tataroglu, A.G. Al-Sehemi, M. Özdemir, R. Özdemir, et al., Frequency and electric field controllable photodevice: FYTRONIX device, Physica B 519 (2017) 53–58.

[46] N. Chaudhary, K. Gill, M. Pahuja, S. Rani, et al., Silicon distyryl-BODIPY hybrid photodiode: moving a step ahead from organic interface layer to type II band alignment, J. Alloys Compd. 978 (2024) 173389.

[47] A.O. Tezcan, S. Eymur, E. Tasci, M. Emrullahoglu, N. Tugluoglu, Investigation of electrical and photovoltaic properties of Au/n-Si Schottky diode with BOD-Z-EN interlayer, J. Mater. Sci. Mater. Electron. 32 (2021) 12513–12520.

[48] Y. Badali, A. Nikravan, S. Altindal, I. Uslu, Effects of a thin Ru-doped PVP interface layer on electrical behavior of Ag/n-Si structures, J. Electron. Mater. 47 (2018) 3510–3520.

[49] G. Aslanbas, P. Durmus, S. Altindal, Y. Azizian-Kalandaragh, The current-voltage (I-V) characteristics and low-high impedance measurements (C/G-V) of Au/(AgCdS:PVP)/n-Si Schottky diode (SD) at dark and under illumination conditions, J. Mater. Sci. Mater. Electron. 35 (2024) 2278.

[50] E.H. Nicollian, J.R. Brews, MOS/metal Oxide Semiconductor/Physics and Technology, 1982.

[51] Ü. Akin, Ö. Yüksel, E. Tasci, N. Tugluoglu, Fabrication of a new hybrid coronene/n-Si structure by using spin coating technique and its photoresponse and admittance spectroscopy studies, Silicon 12 (2020) 1399–1405.

[52] S. Cavdar, Y. Demirolmez, N. Turan, H. Koralay, et al., Investigation of trap states, series resistance and diode parameters in Al/Gelatin/n-Si Schottky diode by voltage and frequency dependent capacitance and conductance analysis, ECS J. Solid State Sci. Technol. 11 (2022) 025001.

[53] S. Cavdar, Y. Demirolmez, N. Turan, H. Koralay, N. Tugluoglu, *Analysis of voltage mid frequency-dependent series resistance and interface states of Al/ZnCo2O4: gelatin/n-Si diode*, J. Mater. Sci. Mater. Electron. 33 (2022) 22932–22940.

[54] W.A. Hill, C.C. Coleman, A single-frequency approximation for interface-state density determination, Solid State Electron. 23 (1980) 987–993.

[55] N. Tugluoglu, S. Karadeniz, B. Baris, Analysis of relaxation time and density of interface trap on perylene-diimide (PDI)/p-Si (100) Schottky diodes, Mater. Sci. Semicond. Process. 33 (2015) 199–205.

[56] M. Çakar, A. Türüt, Y. Onganer, The conductance- and capacitance-frequency characteristics of the rectifying junctions formed by sublimation of organic pyronine-B on p-type silicon, J. Solid State Chem. 168 (2002) 169–174.

[57] Ş. Aydoğan, M. Sağlam, A. Türüt, Effect of temperature on the capacitance–frequency and conductance–voltage characteristics of polyaniline/p-Si/Al MIS device at high frequencies, Microelectron. Reliab. 52 (2012) 1362–1366.

[58] S. Alptekin, S.O. Tan, Ş. Altındal, Determination of surface states energy density distributions and relaxation times for a metal-polymer-semiconductor structure, IEEE Trans. Nanotechnol. 18 (2019) 1196–1199.

[59] R. Padma, K. Sreenu, V.R. Reddy, Electrical and frequency dependence characteristics of Ti/polyethylene oxide (PEO)/p-type InP organic-inorganic Schottky junction, J. Alloys Compd. 695 (2017) 2587–2596.

[60] M. Sharma, S.K. Tripathi, *Frequency and voltage dependence of admittance characteristics of Al/Al2O3/PVA:n-ZnSe Schottky barrier diodes*, Mater. Sci. Semicond. Process. 41 (2016) 155–161.

[61] G. Ersöz, I. Yücedag, Y. Azizian-Kalandaragh, I. Orak, S. Altindal, Investigation of electrical characteristics in Al/CdS-PVA/p-Si (MPS) structures using impedance spectroscopy method, IEEE Trans. Electron. Dev. 63 (2016) 2948–2955.

[62] M. Ulusoy, Y. Badali, G. Pirgholi-Givi, Y. Azizian-Kalandaragh, S. Altindal, The capacitance/conductance and surface state intensity characteristics of the Schottky structures with ruthenium dioxide-doped organic polymer interface, Synth. Met. 292 (2023) 117243.

[63] A. Buyukbas-Ulusan, I. Tasçioglu, A. Tataroglu, F. Yakuphanoglu, S. Altindal, A comparative study on the electrical and dielectric properties of Al/Cd-doped ZnO/p-Si structures, J. Mater. Sci. Mater. Electron. 30 (2019) 12122–12129.

[64] S. Sze, Physics of Semiconductor Devices, Wiley, New York, 1981.